NASA TECHNICAL MEMORANDUM

NASA TM X-2921

NASA TM X-2921

EXPERIMENTAL EVALUATION OF A TF30-P-3 TURBOFAN ENGINE IN AN ALTITUDE FACILITY: EFFECT OF STEADY-STATE TEMPERATURE DISTORTION

by Willis M. Braithwaite

Lewis Research Center
Cleveland, Ohio 44135

NATIONAL AERONAUTICS AND SPACE ADMINISTRATION • WASHINGTON, D. C. • NOVEMBER 1973

1. Report No. NASA TM X-2921	2. Government Accession No.	3. Recipient's Catalog No.
4. Title and Subtitle EXPERIMENTAL EVALUATION OF A TF30-P-3 TURBOFAN ENGINE IN AN ALTITUDE FACILITY: EFFECT OF STEADY-STATE TEMPERATURE DISTORTION		5. Report Date November 1973 6. Performing Organization Code
7. Author(s) Willis M. Braithwaite		8. Performing Organization Report No. E-7499 10. Work Unit No. 501-24
9. Performing Organization Name and Address Lewis Research Center National Aeronautics and Space Administration Cleveland, Ohio 44135		11. Contract or Grant No. 13. Type of Report and Period Covered Technical Memorandum
12. Sponsoring Agency Name and Address National Aeronautics and Space Administration Washington, D.C. 20546		14. Sponsoring Agency Code
15. Supplementary Notes		

16. Abstract

An experimental investigation was conducted to determine the effects of circumferential distortion of the total temperature entering 25, 50, and 75 percent of the inlet circumferential annulus of a turbofan engine. Complete compressor stall resulted from distortions of from 14 to 20 percent of the face averaged temperature. Increasing the temperature level in one sector resulted in that sector moving toward stall by decreasing the equivalent rotor speeds while the pressure ratio remained approximately constant. Stall originated as a rotating zone in the low-pressure compressor which resulted as a terminal stall in the high-pressure compressor. Decreasing the Reynolds number index to 0.25 from 0.5 reduced the required distortion for stall by 50 percent for the conditions investigated.

17. Key Words (Suggested by Author(s))	18. Distribution Statement
Turbofan engine Inlet distortion- temperature Flow distortion TF30	Unclassified - unlimited

19. Security Classif. (of this report)	20. Security Classif. (of this page)	21. No. of Pages	22. Price*
Unclassified	Unclassified		Domestic, $3.00 Foreign, $5.50

* For sale by the National Technical Information Service, Springfield, Virginia 22151

EXPERIMENTAL EVALUATION OF A TF30-P-3 TURBOFAN ENGINE IN AN ALTITUDE FACILITY: EFFECT OF STEADY-STATE TEMPERATURE DISTORTION

by Willis M. Braithwaite

Lewis Research Center

SUMMARY

An experimental investigation was conducted using a gaseous hydrogen burner in front of a TF30-P-3 turbofan engine in an effort to increase the knowledge of the effects of inlet temperature distortion on engine performance. Data were obtained over several rotor speeds and at several Reynolds number indices (RNI) of 0.5, 0.35, and 0.25. Circumferential square-wave patterns of above average temperature extending 90°, 180°, and 270° were investigated.

A temperature difference of from 14 to 20 percent of the average resulted in compressor stall for the conditions investigated. Increasing the temperature distortion shifted the operating point of the fan and low-pressure compressor to lower equivalent speeds and airflows and also to lower temperature and pressure ratios. This resulted in rotating stall in the low-pressure compressor followed by terminal stall originating in the high-pressure compressor. This terminal stall resulted from the combined pressure and temperature distortions entering the high-pressure compressor.

INTRODUCTION

A major problem in the development of some aircraft propulsion systems has been the detrimental effect of inlet-flow distortion on the engine stability limits. Many studies have been made of the effects of pressure distortions on engine stability limits. Fewer studies have been directed toward understanding of the effects of inlet-temperature distortion. These distortions can result from ingestion of exhaust gas from armament firing, or from the exhaust from other engines, for example, ground operation and VTOL-STOL applications (refs. 1 to 3).

To increase the knowledge of the effects of inlet distortions on engine performance and stability limits, a series of experimental programs have been conducted at the NASA Lewis Research Center (refs. 4 to 6). One of these programs reported herein, was concerned with the effect of steady-state temperature distortions on performance and stall limits. A gaseous hydrogen preheater was used upstream of the engine to provide the one-per-revolution circumferential temperature distortion. A two-spool turbofan, typical of those being used or planned for use in modern aircraft, was used for this investigation. High-response pressure instrumentation was used to determine the origin and sequence of stall through the compressor system.

Data are presented for circumferential one-per-revolution distortions of 90°, 180°, and 270° extents and for Reynold's number indices (RNI) of 0.50, 0.35, and 0.25. The results are presented in terms of the stall limits and changes in performance parameters resulting from increasing distortion levels for low rotor mechanical speeds of 68, 73, 84, and 90 percent of the military speed (9525 rpm). The results are compared with the predicted values obtained from use of the parallel compressor theory.

APPARATUS

The engine used for this investigation was a production TF30-P-3 twin-spool turbofan engine. It was installed in an altitude test chamber. The installation was a conventional direct-connect type as shown in figure 1. The engine and instrumentation locations are also shown in this figure and are the same as those described in reference 6, with the addition of a temperature measuring station at the engine inlet. A more complete discussion of the high-response pressure instrumentation design required to obtain 500-hertz frequency response is given in reference 7.

The inlet-temperature distortions were generated by a gaseous hydrogen burner located upstream of the inlet duct bellmouth. This burner was similar to the one described in reference 8. Figure 2 presents photographs of the burner and figure 3 is a schematic of the installation. The total engine airflow passed through the burner, which was divided into four 90° sectors. Each sector could be controlled independently. Each sector contained five annular gutters supported by one crossflow radial gutter. Hydrogen was fed through tubes in these gutters. Five swirl cans in each quadrant provided the ignition source for the main combustors. Temperature control was accomplished by throttling the hydrogen flow into the desired sectors. Differential throttling created the distortions.

PROCEDURE

The minimum temperature distortions, which resulted in stall, were obtained by slowly increasing the gaseous hydrogen flow, and thus temperature, into the selected quadrants of the preheater until compressor stall occurred. The temperature in those quadrants were observed at the time of stall. These same condions were re-established with the 12th stage bleeds open, permitting stall-free operation with the previously observed temperature distortion. Steady-state data were recorded to provide a more detailed evaluation of the flow conditions at the engine inlet that resulted in stall. The steady-state data acquisition systems are described in reference 9. Data were also recorded on an analog tape system during the slow transient into stall permitting the calculation of pressure ratios and the determination of the stall sequence

Steady-state data were also obtained at at least two intermediate levels of temperature distortion in addition to that required to stall the engine. These data permitted the evaluation of the effects on steady-state performance of increasing distortion.

The airflow and rotor speeds are presented in this report as ratios to the standard sea-level military values for this particular engine. These base values used are low rotor speed, $N_L/\sqrt{\theta_2} = 9525$ rpm and $W_{at}\sqrt{\theta_2}/\delta_2 = 107$ kilograms per second. For the high-pressure compressor, $N_H/\sqrt{\theta_3} = 10\,360$ rpm and $W_{ac}\sqrt{\theta_3}/\delta_3 = 12.9$ kilograms per second. The data were measured in U.S. Customary Units and then converted to the SI units (ref. 10). All symbols are defined in the appendix.

The total inlet airflow was computed from measurements made at the engine face (station 2) since the normal airflow station (station 1) was obstructed by the preheater. The engine inlet station had previously been calibrated against station 1 without the preheater. The core airflow was calculated from measurements made at the high-compressor inlet (station 3), which also had previously been calibrated against the engine fuel flow and the overall engine heat balance. Basic one-dimensional flow equations were used in these calculations.

Data are presented for increased temperature levels in one, two, and three quadrants, that is, 90°, 180°, and 270° circumferential extents. The inlet total pressure was set at three levels: 0.5, 0.35, and 0.25 atmospheres. The temperature in the unheated quadrants was maintained at ambient and thus the RNI in the unheated sectors was 0.5, 0.35, and 0.25. A ram pressure ratio of approximately 3 was maintained across the engine during this investigation.

RESULTS AND DISCUSSION

To gain an insight into the effects of inlet total temperature distortion on the performance of the compressor system, data were obtained with circumferential square wave patterns of 90°, 180°, and 270° extents at a RNI of 0.5. Data were also obtained at values of RNI of 0.35 and 0.25 with an extent of 180°. The results are discussed in six catagories: the inlet profiles, the distortion limits, a history of stall, the effect on overall performance, the effect on the compressor operating points, and the parallel compressor model.

Inlet Profiles

Typical circumferential profiles of total temperature, total pressure, and axial velocity are presented in figure 4 for extents of 90°, 180°, and 270°. These profiles are based on the average of the five radial measurements at each angular position (fig. 1). Less than 1-percent pressure distortion is observed for these conditions. An approximately 6-percent increase in velocity occurred in the heated sector. The temperature levels in the heated sector required to stall the engine were from 15 to 20 percent above the unheated level.

The radial variations of these parameters can be seen on the contour maps (fig. 5). Little radial variation is seen in the total temperature (figs. 5(a) to (c)). The decrease in total pressure and velocity due to the boundary layers on the inner and outer walls are the only major radial variation observed in figures 5(d) and (e). The distortions were basically square-wave circumferential patterns of total temperature distortion. Thus the variations in performance were due to these distortions.

Gas passing through a compressor does not necessarily follow a straight path; that is, a particle entering at the top-dead center does not necessarily exit at top-dead-center. The instrumentation in the compressor for these tests was insufficient to determine the amount of rotation. However, unreported temperature pattern data obtained during pressure distortion testing indicated that the temperature pattern rotated about 90° to 100° in the direction of rotor rotation in passing through the low-pressure compressor (LPC) for a 90 percent low rotor speed, figure 6, and an additional 50° in the high-pressure compressor (HPC). These data are in good agreement with those predicted by the engine manufacturer, as is noted in the figure. Other evidence of the rotation is that the calculated efficiencies for the LPC on the side behind the heated inlet sector were high (for one case, 110 percent), while low on the other side (72 percent). Using the average values of pressure and temperature resulted in an efficiency of 88 percent (nearly normal).

Assuming 90° rotation in the LPC, the instrumentation layout (fig. 6) indicated that the total-pressure measurements at station 3 at 116° would be in the heated flow and that the total temperature at 60° would be in the unheated flow and thus "undistorted." Likewise, the total temperature and total pressure at 260° became "distorted." At the high-pressure compressor exit (station 4), the values at 80° and 120° became "undistorted" and those at 300° became "distorted." Many of these measurements are in the edge regions of the distortion patterns.

Distortion Limits

The temperature distortion levels resulting in compressor stall are shown in figure 7. The values of distortion are shown as functions of the circumferential extent ψ_T, equivalent low rotor speed, and Reynolds number index. The definition of distortion used in this report is the difference in temperature as a percent of the face average temperature. For a square-wave it is the average of the high minus the average of the low divided by the face average temperature.

There was little or no difference in the distortion required to stall the compressor with either the 90° or 180° extents. The 270° extent, however, required approximately a 2-percentage-point increase in distortion level. The 90° and 180° extent temperature distortions required approximately an 18-percent distortion level to stall the engine with 90 percent low rotor speed at 0.5 RNI. A 20 to 23 percent distortion, depending on extent, can be estimated as being required to stall the engine with a 100 percent speed. Rotor speeds between 90 and 100 percent were not investigated in as much as the higher inlet temperature could have resulted in an overspeed condition and the lower speed minimized the turbine-inlet temperature overshoot.

The distortion required to stall the compressor system decreased with RNI from 18 percent at 0.5 to 8.5 percent at 0.25 at 88 percent low rotor speed. The trend with Reynolds number index is not linear in as much as there is less effect at the higher indices. The increase in distortion required above the 0.5 index would be very small; therefore, the distortion level required at sea-level would be about the same as for the 0.5 index.

History of Stall

The time histories of the pressures and pressure ratios down both sides of the engine are presented for a stall sequence in figure 8. The sides are designated as right or $90^{\circ}\pm90^{\circ}$ (behind the inlet distortion) and left or $270^{\circ}\pm90^{\circ}$ (behind the undistorted

side of the inlet). The sequence of events is as follows. First an indication of rotating stall can be observed on the right hand side pressure trace for station 2.3 (indicated by I). This would be in the heated air. The rotating stall can also be seen in the static pressure at station 2.6 (II). These indications of rotating stall are evident in the total-pressure ratios of the fan and low-pressure compressor (fig. 8(b)). These stall zones grow as indicated by the static pressure at station 2.3 (III). This was followed by a loss in total pressure on the right side at station 3 (IV). This loss coupled with the rise in total pressure at the same time at station 2.3 indicates that the stall occurred between these stations.

The rotating stall was followed by breakdown of the flow starting on the left side at station 3.12 (middle of the high-pressure compressor, indicated in fig. 8 by V). This flow breakdown then rotated to the right side of the compressor and resulted in terminal stall. The apparent breakdown in flow in the left side behind the cool sector of the inlet may not be contradictory if the air rotated the 90° to 100° indicated by the pressure distortion data, as mentioned previously.

Effects on Performance

Total temperature distortion of the flow entering the compressor resulted in a reduction of the Reynolds number and equivalent low rotor speed in the heated zone. Some rematching of the compressor units may also have occurred. As described in the Procedure section, the total pressure and temperature were held constant over one part of the engine face, while the total temperature was raised in front of the other side of the face. Therefore, the Reynolds number index decreased from 0.5 in the unheated sector to 0.4 in the heated sector for a 180° distortion of 18 percent. Based on face average pressure and temperatures, the Reynolds number index was 0.44 (fig. 9(a)). Therefore, it is assumed that this reduction in RNI would be accompanied by normal changes in performance and distortion tolerance of the compressor systems.

The equivalent low rotor speed in the heated inlet sector decreased 8.7 percent, while the mechanical speed was constant. However, the decrease was 4 percent based on face averaged temperature for the 18-percent distortion of 180° extent (fig. 9(b)). A decrease in equivalent low rotor speed for an engine operating with no distortion would result in a decrease in performance. The 4 percent decrease in low rotor speed resulting from the 18-percent 180° temperature distortion would be expected to result in an approximately 6-percent decrease in engine total pressure ratio and an 11-percent decrease in overall compressor pressure ratio.

To eliminate the effects on performance due to the reduction in equivalent speed, a ratio of the parameters presented in figure 9(c) to (e) to the value of that parameter

for the engine operating with no inlet distortion at the same average equivalent low rotor speed was formed. The overall engine total perssure ratio, the overall compressor total pressure ratio, and the total inlet airflow were observed to be independent of the temperature distortion (fig. 9).

Compressor Performance

The TF30 compressor system has three basic components; the fan, the low-pressure compressor, and the high-pressure compressor. Each unit is defined by a total pressure ratio, an equivalent inlet mass flow, and an equivalent rotor speed. These are, as used in this report for the fan $P_{2.3F}/P_2$, $W_{at}\sqrt{\theta_2}/\delta_2$, and $N_L/\sqrt{\theta_2}$; for the LPC P_3/P_2, $W_{ac}\sqrt{\theta_2}/\delta_2$, and $N_L/\sqrt{\theta_2}$; and for the HPC P_4/P_3, $W_{ac}\sqrt{\theta_3}/\delta_3$, and $N_H/\sqrt{\theta_3}$. The parameters that describe the match between the fan and the LPC are the bypass ratio and the equivalent core airflow. The parameter that describes the match between the LPC and the HPC is the relation of equivalent low and high rotor speeds. The effect of increasing the temperature distortion on these matching parameters is shown in figure 10. There is an indicated increase in bypass ratio suggesting that, for the same total airflow, more air is going into the fan duct and less into the core. The high rotor speed also increases with increasing distortion. Thus increasing the temperature distortion decreased the indicated equivalent core airflow and increased the bypass ratio and the equivalent high rotor speed.

The effects of inlet temperature distortion on the fan and compressor operating points are shown on the maps of figure 11. Data based on the averaged conditions are presented for increasing levels of 180° extent temperature distortion for low rotor speeds of 73, 84, and 90 percent of military. Increasing the level of distortion at constant mechanical speed shifted the operating points of the fan and LPC to lower equivalent airflows and total pressure ratios along the normal operating lines. Since the core airflow decreased with distortion, the equivalent speed lines shifted to lower equivalent airflows on the LPC map (fig. 11(b)).

The indicated effects of the temperature distortion on the HPC were somewhat different (fig. 11(c)). The operating point moved to lower equivalent airflows at a constant pressure ratio. Again, the equivalent speed lines moved to lower equivalent airflows. As mentioned previously, the effects of the rotation of the heated airflow through the compressor on the measurement accuracy at station 3 and through the HPC on those at station 4 are not known. Therefore, caution must be used in interpreting these data. This will be discussed more fully in the next section.

Theoretical Model

The effects of inlet-flow distortion on a simple compressor can be modeled satisfactorily by the parallel compressor theory. The best agreement is obtained with a sharply defined square-wave circumferential distortion. This theory is used extensively in reference 11. Close agreement would not be expected for a complicated compressor like the TF30 where the bypass flow and the match between the rotors may be influenced by the distortion. Trends can be determined, however.

The parallel compressor theory states that a compressor operating with a simple one-per-revolution circumferential distortion may be considered as being composed of two individual compressors operating in parallel, each with different inlet conditions, one corresponding to the distorted side and the other to the undistorted side. The performance of each "parallel" compressor may be defined using the compressor map for the undistorted compressor. Further, no crossflow may occur between these parallel compressors. The relatively large volumes at the exits of the compressors and fan allow the static pressures to become uniform in these areas. Therefore, if the distortion is only thermal, the total pressure at the engine inlet will be uniform and thus the exit static to inlet total pressure ratios for both the "heated" and "unheated" compressors will be the same for the fan and the LPC.

The performance was predicted for a 15-percent temperature distortion with the TF30. The heated air temperature was used to determine the equivalent low rotor speed on the distorted side, and the temperature of the unheated air was used to determine the equivalent low-rotor speed in the undistorted side of the fan and LPC. The static to total fan and LPC pressure ratios based on the average equivalent low rotor speed were used for both of the parallel fans and for the parallel LPCs. The results are presented in figure 12 together with measured data. The data and theory are presented as ratios to the corresponding values with the engine operating at the same averaged equivalent low rotor speed (87 percent of military) without inlet distortion.

The measured temperatures show less divergence from the undistorted data than those predicted by the parallel compressor theory. The difference between measured and theoretical values increases as the air passes through the compressor. As mentioned previously, the pattern of distortion probably rotates in passing through the compressor and therefore the measured values are indicative of neither the heated nor the unheated airflow. A discrepency exists between the theoretical values as determined by the parallel compressor theory and measured Mach numbers at station 2. A possible explanation for this may be the 28 centimeters that the instrumentation station is ahead of the first-stage rotor. Thus, if a static-pressure gradient exists in front of the engine face, the station 2 values would be low compared with the face values.

The parallel compressor theory indicates that the mechanism of stall with circum-

ferential temperature distortion was the decrease in equivalent rotor speed in the heated compressor, while the pressure ratio is determined by the averaged conditions at the inlet and exit of the parallel compressors. Thus the heated flow compressor produced the same pressure ratio as the unheated compressor but at a lower equivalent speed and airflow. Stall resulted in the heated compressor when the equivalent speed and airflow were reduced sufficiently by increasing the inlet temperature. In the case of a twin-spool engine, a circumferential total pressure profile (distortion) may also develop at the inlet of the second spool. The matching criteria are the equivalent airflow from the LPC into the HPC and the static to total HPC pressure ratio obtained from the overall and the LPC total pressure ratios.

The predicted operating points for a 15-percent distortion are presented on the performance maps of figure 13. In general the movement of the operating points based on the averaged conditions is similar to that observed with the measured data on figure 11. A second set of operating points are also presented in the figure for a 21-percent distortion. This was the predicted distortion required to stall the compressor system. The approximately 3-point increase in distortion above that required to stall the compressor at 90 percent low rotor speed (fig. 7) can probably be attributed to neglecting the decrease in RNI in the distorted sector and variations in BPR and rotor speed match in this simplified analysis.

Both the heated LPC and HPC are observed to be operating close to their stall lines (fig. 13). It is plausible that rotating stall developed in the LPC at these conditions and that the additional flow distortion at the high-pressure compressor inlet resulting from the rotating stall was sufficient to stall the HPC.

SUMMARY OF RESULTS

An experimental investigation was conducted to obtain a better understanding of the effects of inlet-temperature distortion on the performance of a turbofan engine. This report presents the results of slowly increasing the total temperature in one sector of the inlet of the TF30 engine. The following results were obtained:

1. Stall resulted from 14 to 20 percent temperature distortions at a Reynolds number index of 0.5 for the range of speeds and extents investigated. This would be approximately a 40° to 56° C temperature increase over the unheated side.

2. The distortion required to stall the TF30 decreased as the Reynolds number index decreased. It went from a value of 18 percent for a 180° square wave at 0.5 to 8.5 percent at 0.25 RNI.

3. The part of the compressor behind the heated inlet sector operated at the same static to total pressure as that behind the unheated inlet sector but at reduced equiv-

alent rotor speeds and equivalent airflows. This forced the heated side toward stall. A parallel compressor analysis indicated that both LPC and the HPC were on the verge of stall with the limiting temperature distortion.

4. Flow breakdown was observed to begin with a rotating stall zone in the low-pressure compressor, which was followed by terminal stall in the high-pressure compressor.

5. There were strong indications that the temperature distortion pattern rotated as much as 140^{o} in the direction of rotor rotation in passing through the compressor system. Therefore, care must be taken in interpreting these results for the high-pressure compressor.

Lewis Research Center,
National Aeronautics and Space Administration,
Cleveland, Ohio, July 27, 1973,
501-24.

APPENDIX — SYMBOLS

BPR	bypass ratio, W_{aF}/W_{aC}
CPR	overall compressor total pressure ratio, P_4/P_2
EPR	engine total pressure ratio, P_7/P_2
HPC	high-pressure compressor
LPC	low-pressure compressor
M	Mach number
N	rotor speed, rpm
P	total pressure, N/cm^2, abs
p	static pressure, N/cm^2, abs
RNI	Reynolds number index, $\delta/\varphi\sqrt{\theta}$
T	total temperature, K
V	velocity, cm/sec
W	mass flow rate, kg/sec
δ	P/P_{sl}
θ	T/T_{sl}
μ	absolute viscosity, (kg) (sec)/cm^2
φ	μ/μ_{sl}
ψ	circumferential location from top center, deg
ψ_T	circumferential extent of above average temperature, deg

Subscripts:

a	air
av	average
B	base data obtained with an undistorted inlet at the same average equivalent low rotor speed as the distorted data
c	core part of engine
D	average at specified station when operating with distorted inlet
d	heated airflow section of engine as defined by above average total temperature
F	fan

H	high-speed rotor
L	low-speed rotor
MIL	values at equivalent military condition
sl	standard sea-level conditions
t	total
ud	unheated airflow section of engine as defined by below average total temperature
2, 2.3, 3, etc.	station locations as defined in fig. 1

REFERENCES

1. Felderman, E. J.; and High, M. D.: Missile Exhaust Gas Ingestion Simulation. ARO, Inc. (AEDC-TR-71-252), 1971.

2. Gabriel, David S.; Wallner, Lewis E.; and Lubick, Robert J.: Some Effects of Transients in Inlet Pressure and Temperature on Turbojet Engines. Preprint 709, Inst. Aero. Sci., Jan. 1957.

3. Wallner, Lewis E.; Useller, James W.; and Saari, Martin J.: A Study of Temperature Transients at the Inlet of a Turbojet Engine. NACA RM E57C22, 1957.

4. Werner, Roger A.; Abdelwahab, Mahmood; and Braithwaite, Willis M.: Performance and Stall Limits of an Afterburner-Equipped Turbofan Engine with and without Inlet Flow Distortion. NASA TM X-1947, 1970.

5. McAulay, John E.: Effect of Dynamic Variations in Engine-Inlet Pressure on the Compressor System of a Twin-Spool Turbofan Engine. NASA TM X-2081, 1970.

6. McAulay, John E.; and Abdelwahab, Mahmood: Experimental Evaluation of a TF30-P-3 Turbofan Engine in an Altitude Facility: Afterburner Performance and Engine-Afterburner Operating Limits. NASA TN D-6839, 1972.

7. Armentrout, Everett C.: Development of a High-Frequency-Response Pressure-Sensing Rake for Turbofan Engine Tests. NASA TM X-1959, 1970.

8. Rudey, Richard A.; and Antl, Robert J.: The Effect of Inlet Temperature Distortion on the Performance of a Turbo-Fan Engine Compressor System. NASA TM X-52788, 1970.

9. Staff of Lewis Laboratory: Central Automatic Data Processing System. NACA TN 4212, 1958.

10. Mechtly, E. A.: The International System of Units: Physical Constants and Conversion Factors, Revised. NASA SP-7012, 1969.

11. Melick, H. C., Jr.; and Simpkin, W. E.: A Unified Theory of Inlet/Engine Compatibility. Paper 72-1115, AIAA, Nov. 1972.

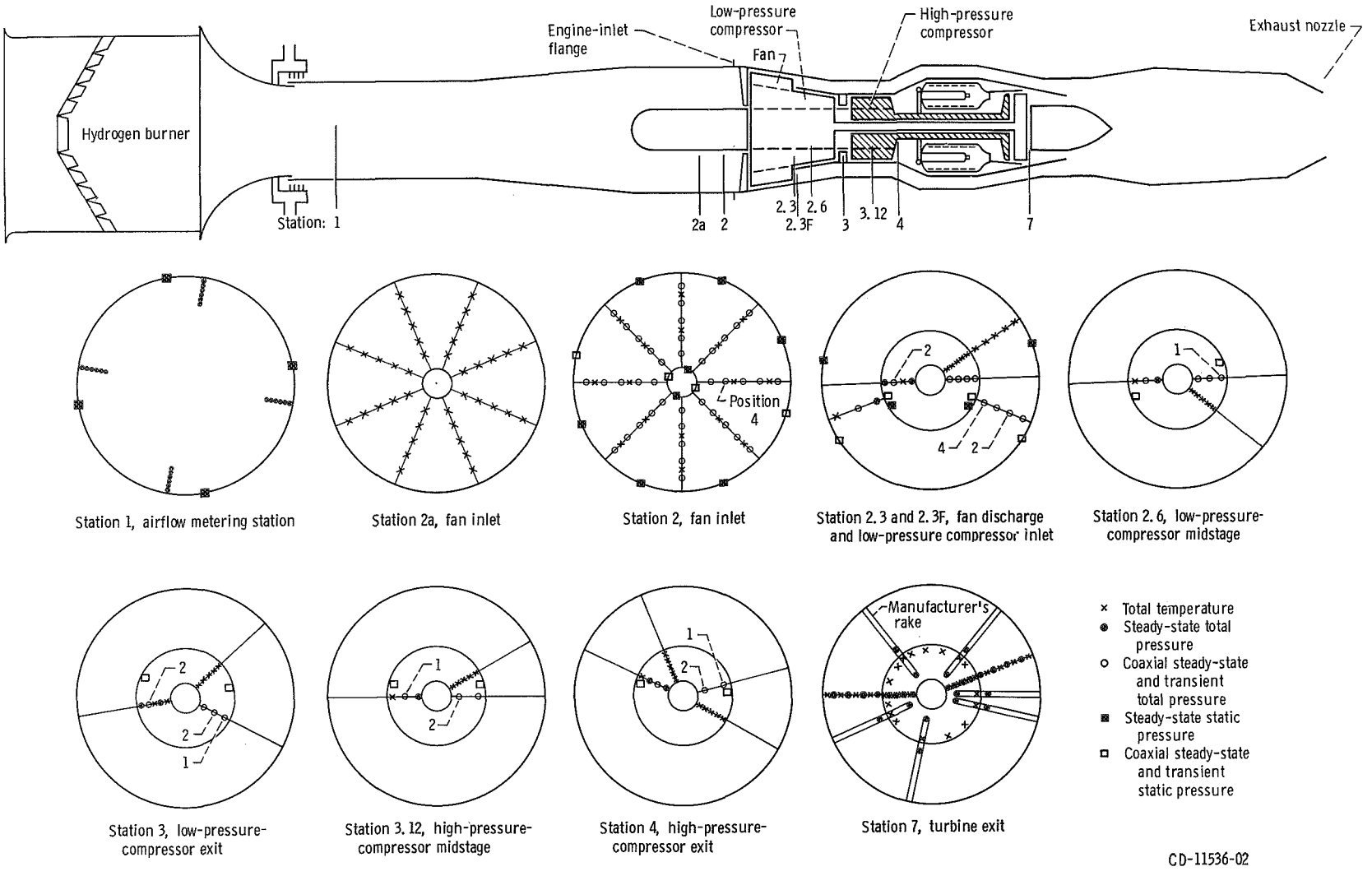

Figure 1. - Instrumentation layout for TF30-P-3 turbofan engine. (Instrumentation stations viewed looking upstream.)

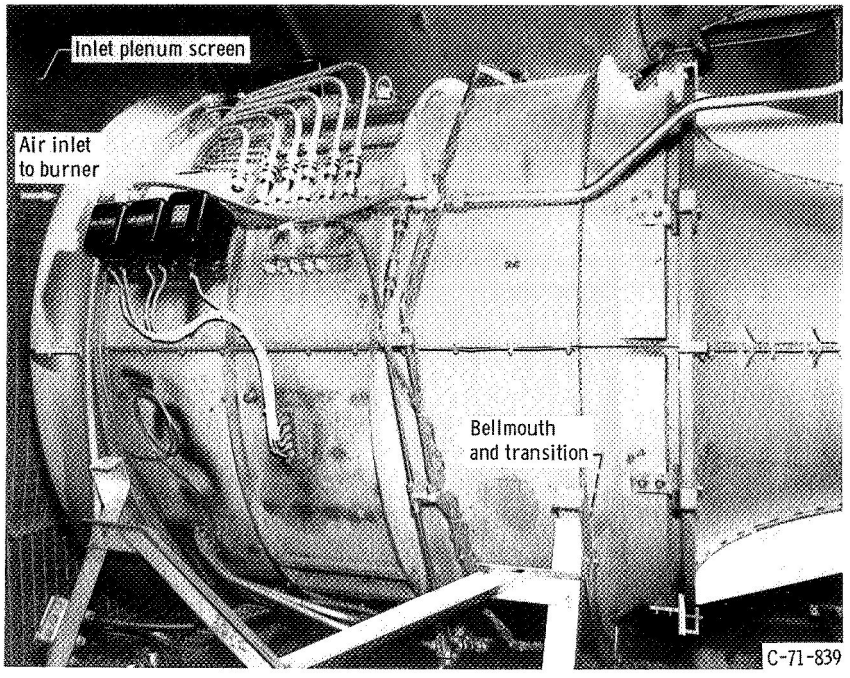

(a) External view.

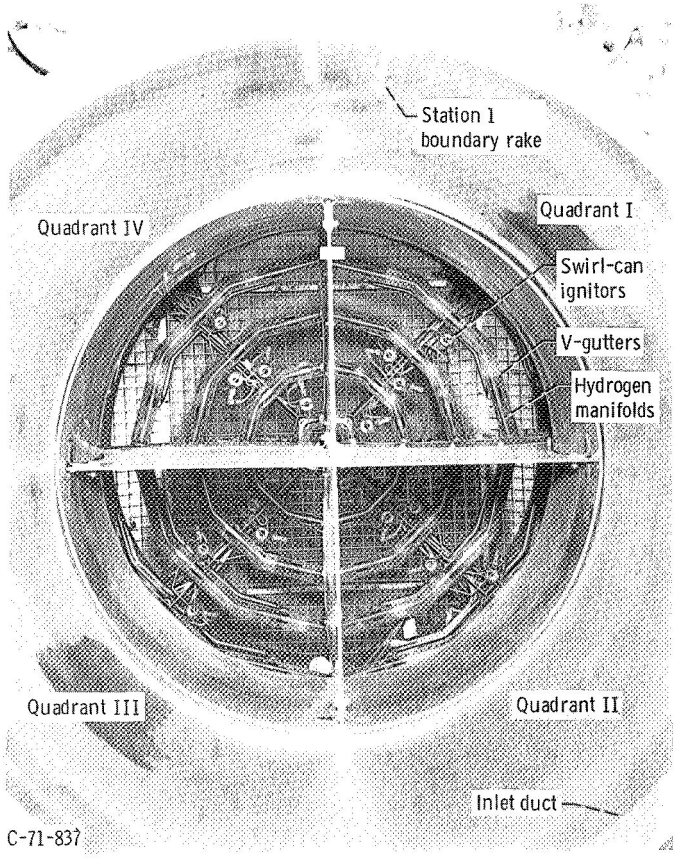

(b) Internal view looking forward.

Figure 2. - Gaseous hydrogen burner installed in altitude chamber.

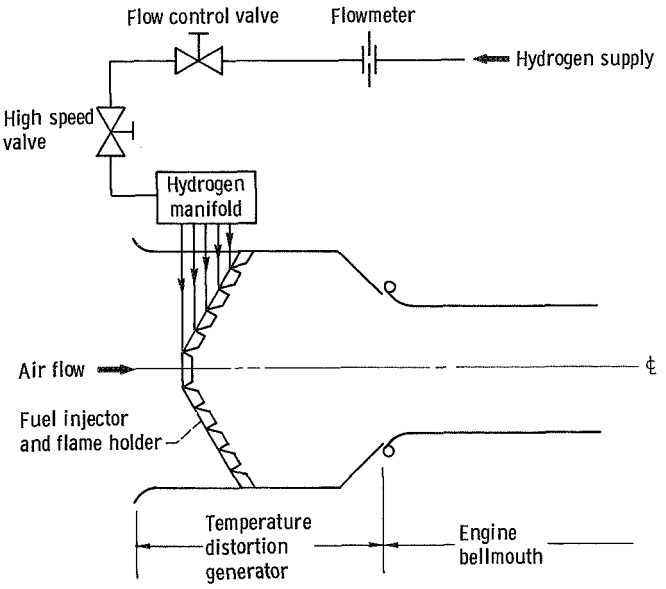

Figure 3. - Hydrogen fueled temperature distortion generator.

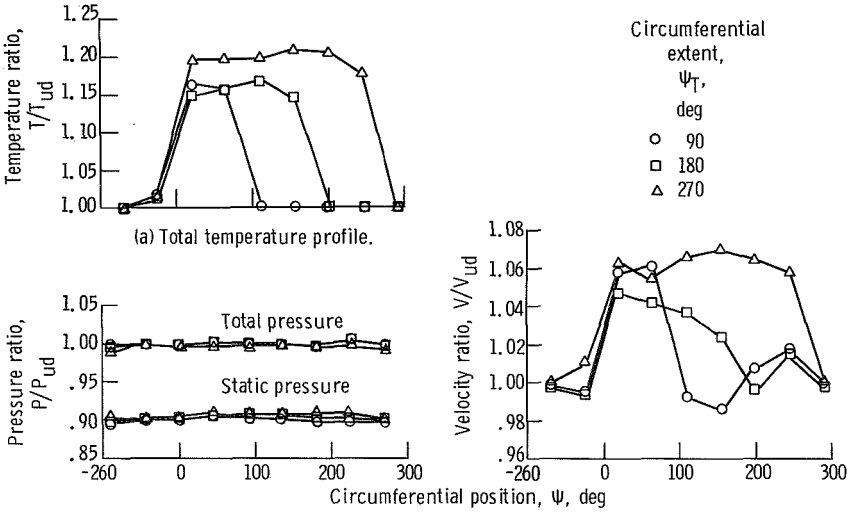

(a) Total temperature profile.

(b) Total and static pressure profiles.

(c) Velocity profiles.

Figure 4. - Rake averaged engine inlet profiles with resulting compressor stall at 84 percent of equivalent low-rotor speed and Reynolds number index of 0.15.

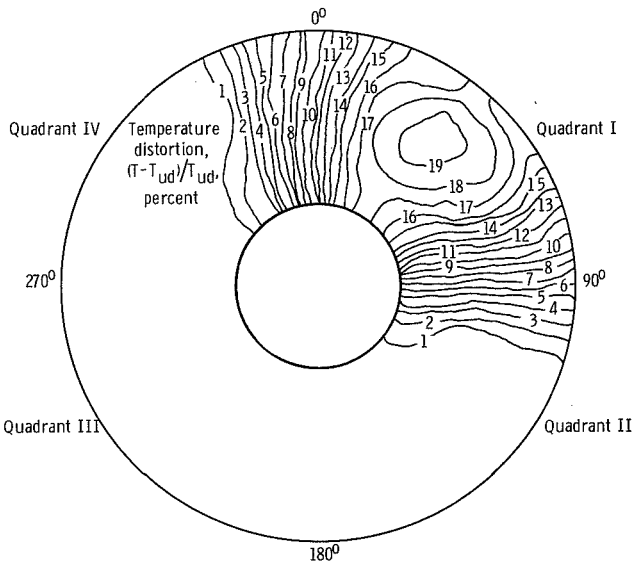

(a) Circumferential extent of temperature distortion, 90°.

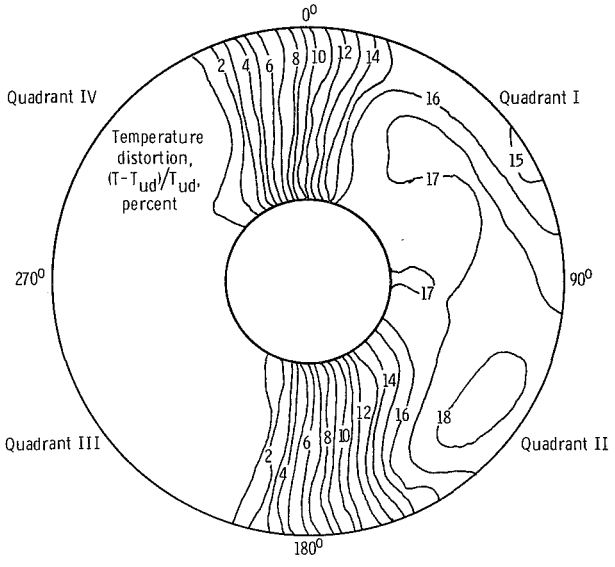

(b) Circumferential extent of temperature distortion, 180°.

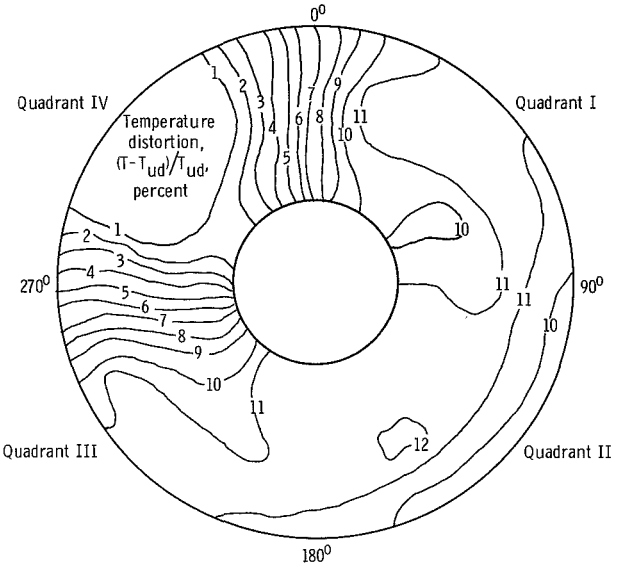

(c) Circumferential extent of temperature distortion, 270°.

Figure 5. - Compressor inlet contour maps for 84 percent low-rotor speed at Reynolds number index of 0.5; stall conditions; looking forward.

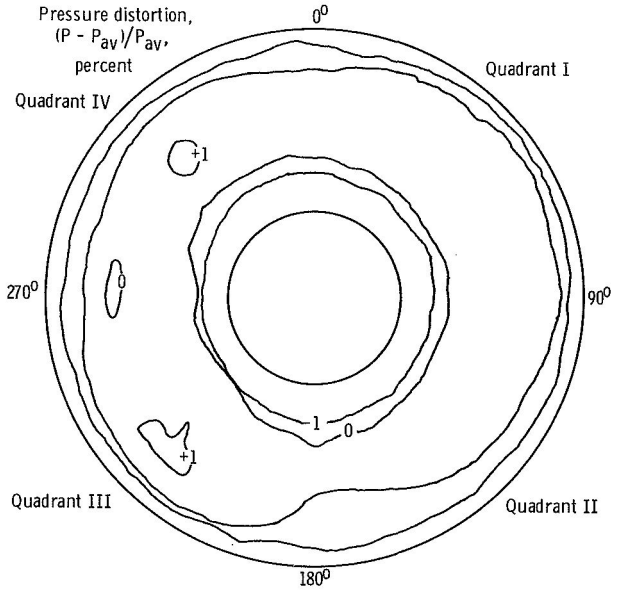

(d) Total pressure variation for 180° extent of temperature distortion.

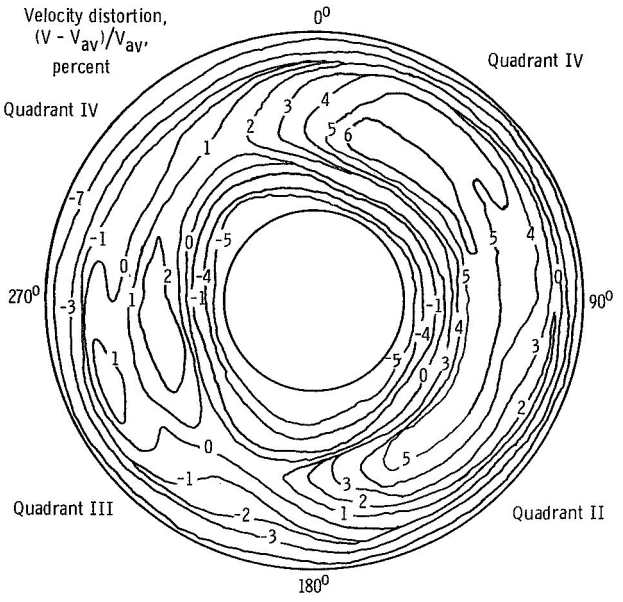

(e) Inlet flow velocity for 180° extent of temperature distortion.

Figure 5. - Concluded.

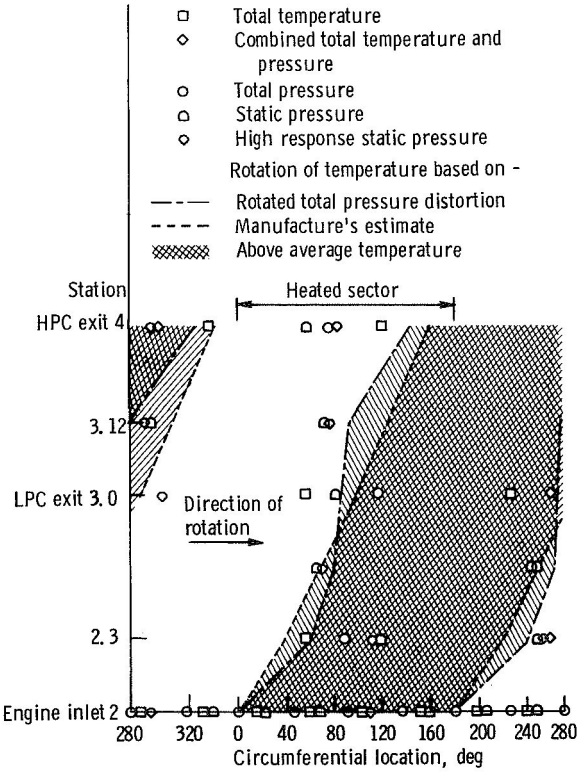

Figure 6. - Estimated rotation of heated airflow in passing through compressor system. Corrected speed, 90 percent of military, low-rotor.

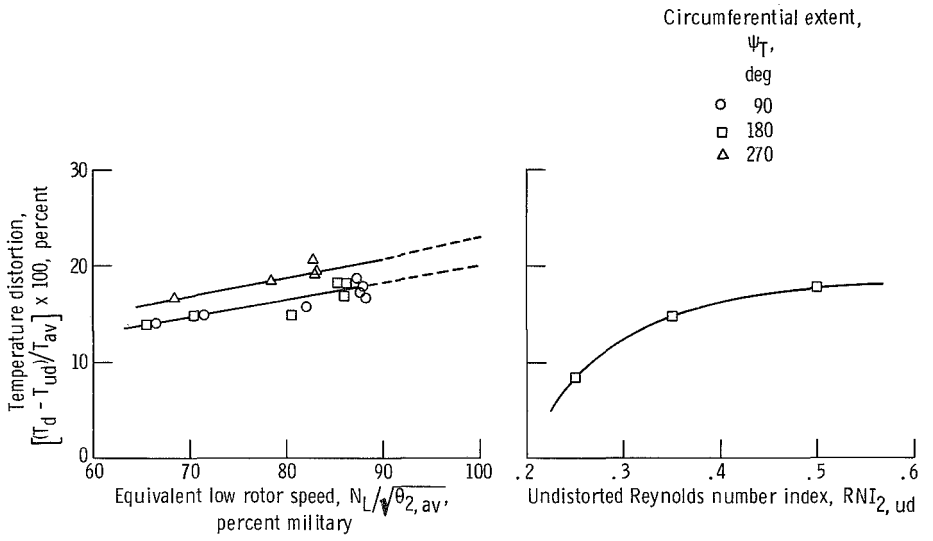

(a) Effect of rotor speed and extent. Undistorted Reynolds number index, 0.5.

(b) Effect of undistorted Reynolds number index. Circumferential extent of temperature distortion, 180^0; corrected low-rotor speed, 88 percent of military.

Figure 7. - Stall limited inlet steady-state temperature distortion for TF30 turbofan engine.

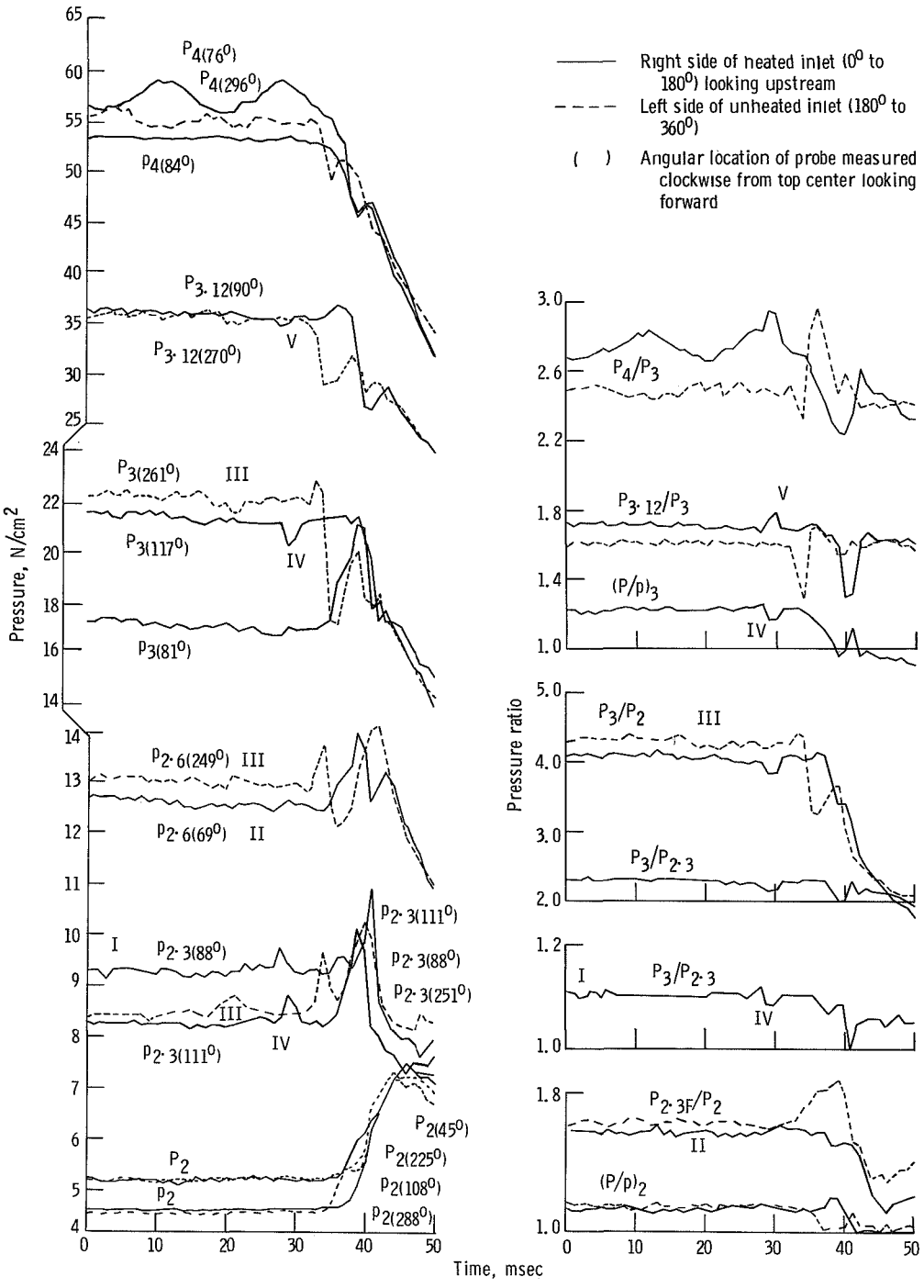

(a) Interstage pressure.

(b) Pressure ratio.

Figure 8. - Pressure time history to stall at 90 percent $N_L/\sqrt{\theta_{2,ud}}$ and Reynolds number index of 0.5 for TF30 turbofan engine with 180° square-wave temperature distortion.

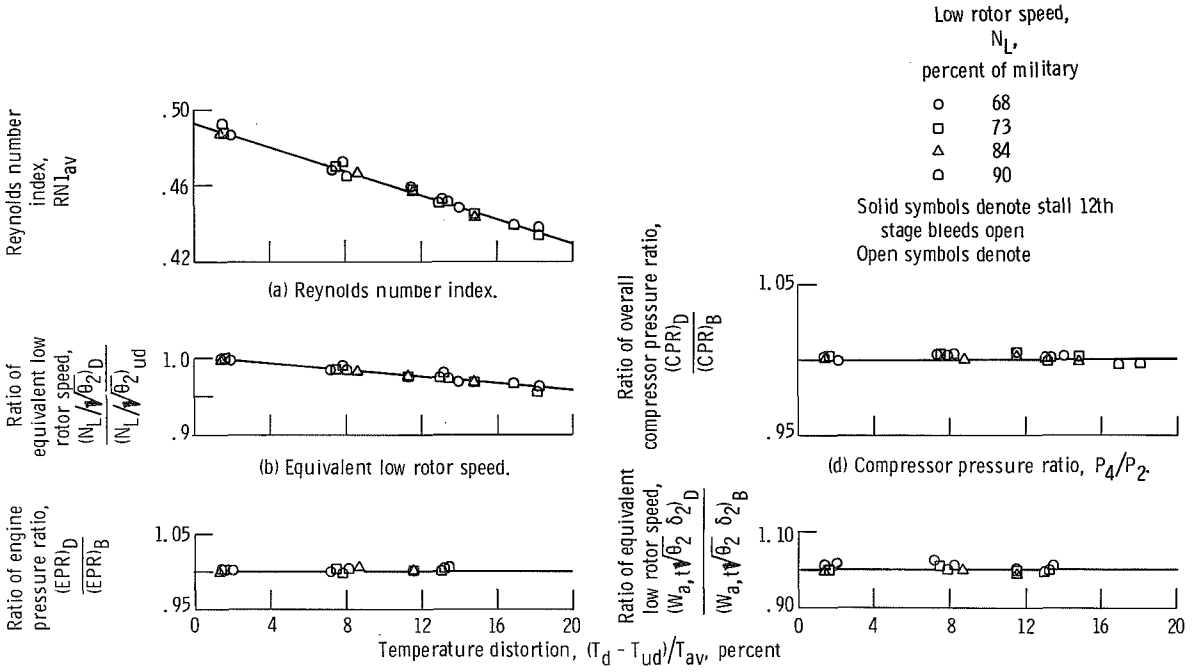

Figure 9. - Effects of inlet total temperature distortion on engine performance. 180^0 Square wave; undistorted Reynolds number index, 0.5.

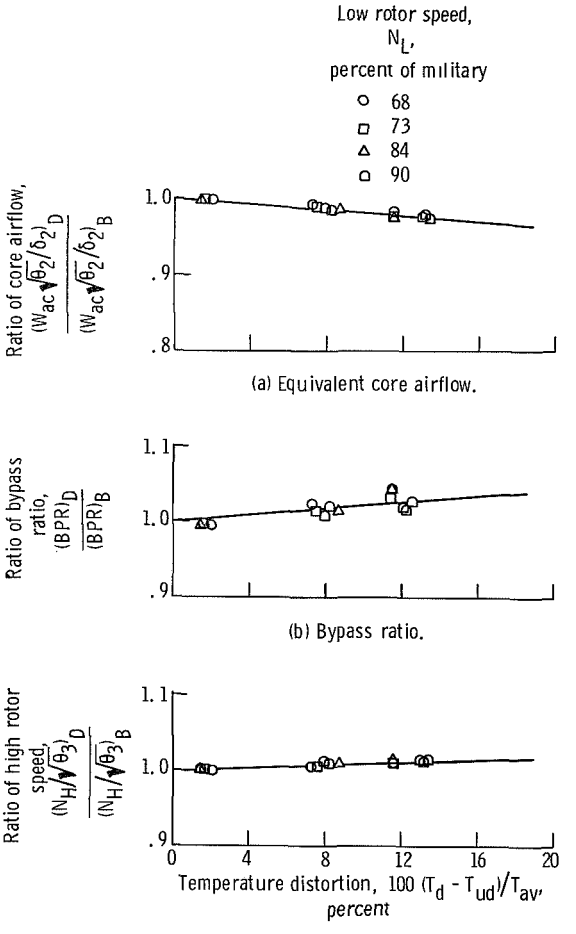

(a) Equivalent core airflow.

(b) Bypass ratio.

(c) Equivalent high rotor speed.

Figure 10. - Effect of inlet total temperature distortion on compressor matching parameters. 180° Square wave; undistorted Reynolds number index, 0.5.

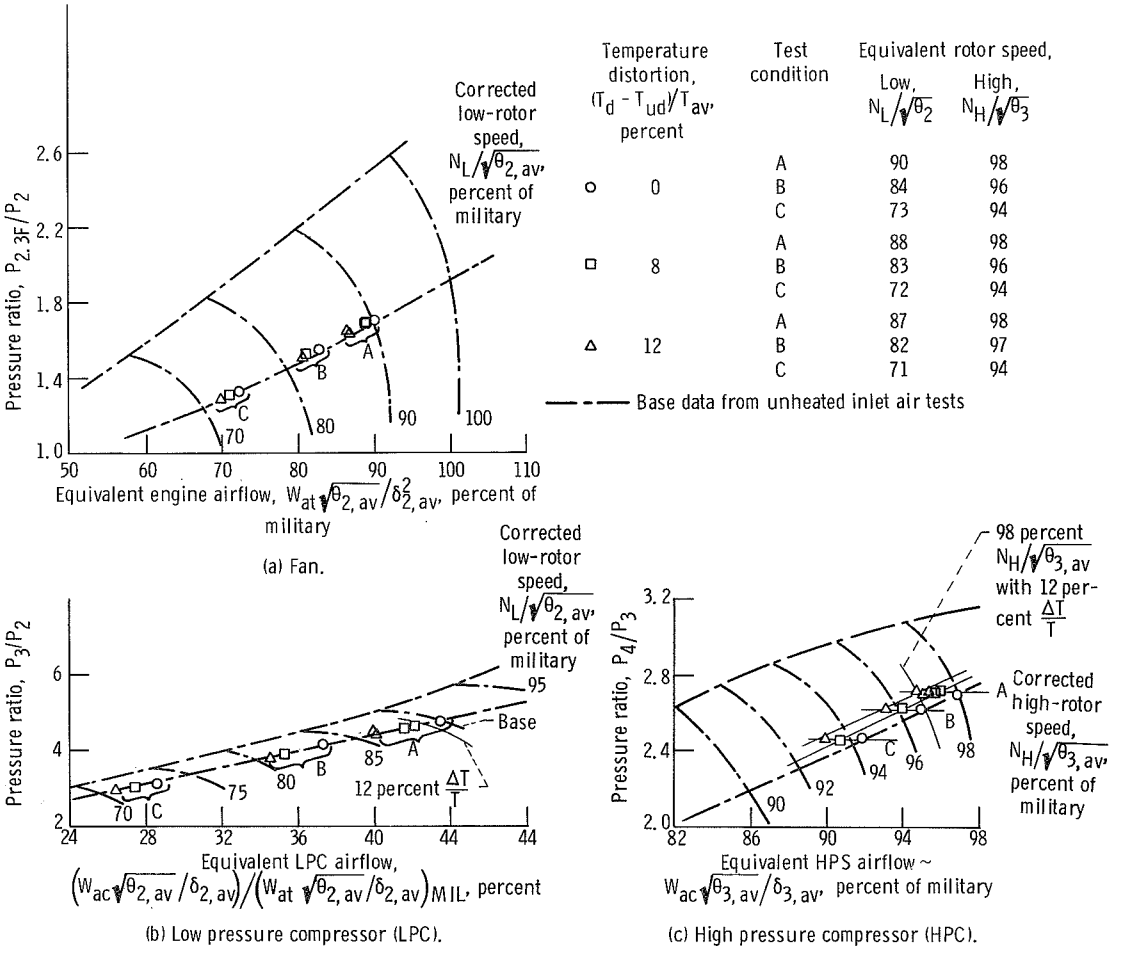

(a) Fan.

(b) Low pressure compressor (LPC).

(c) High pressure compressor (HPC).

Figure 11. - Effects of inlet temperature distortion on fan and compressor performance. Reynolds number index, 0.5; circumferential extent of temperature distortion, 180^0.

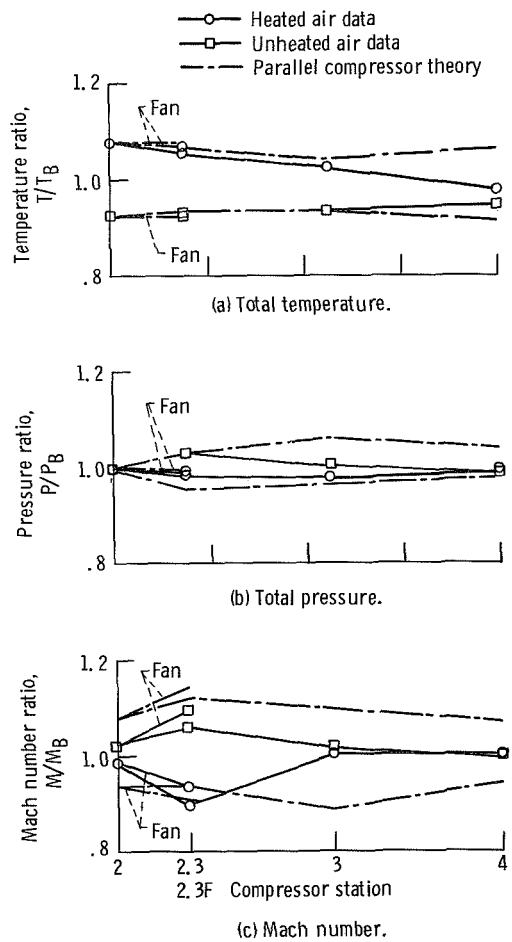

Figure 12. - Effect of inlet temperature distortion on compressor system performance. Corrected low-rotor speed, 87 percent of military; circumferential extent of temperature distortion, 180°, temperature distortion, 15 percent.

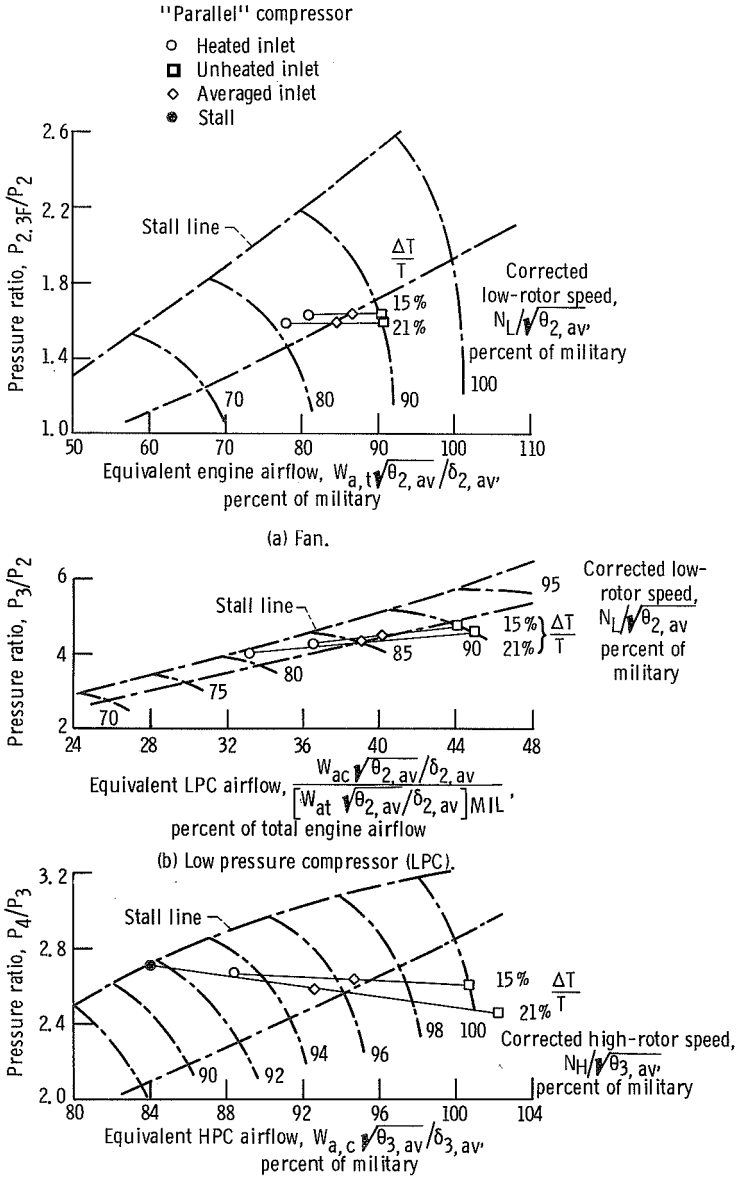

Figure 13. - Operating points predicted by the simplified parallel compressor theory. Low-rotor speed and corrected low-rotor speed, 90 percent; Reynolds number index, 0.5.

"The aeronautical and space activities of the United States shall be conducted so as to contribute . . . to the expansion of human knowledge of phenomena in the atmosphere and space. The Administration shall provide for the widest practicable and appropriate dissemination of information concerning its activities and the results thereof."

—NATIONAL AERONAUTICS AND SPACE ACT OF 1958

NASA SCIENTIFIC AND TECHNICAL PUBLICATIONS

TECHNICAL REPORTS: Scientific and technical information considered important, complete, and a lasting contribution to existing knowledge.

TECHNICAL NOTES: Information less broad in scope but nevertheless of importance as a contribution to existing knowledge.

TECHNICAL MEMORANDUMS: Information receiving limited distribution because of preliminary data, security classification, or other reasons. Also includes conference proceedings with either limited or unlimited distribution.

CONTRACTOR REPORTS: Scientific and technical information generated under a NASA contract or grant and considered an important contribution to existing knowledge.

TECHNICAL TRANSLATIONS: Information published in a foreign language considered to merit NASA distribution in English.

SPECIAL PUBLICATIONS: Information derived from or of value to NASA activities. Publications include final reports of major projects, monographs, data compilations, handbooks, sourcebooks, and special bibliographies.

TECHNOLOGY UTILIZATION PUBLICATIONS: Information on technology used by NASA that may be of particular interest in commercial and other non-aerospace applications. Publications include Tech Briefs, Technology Utilization Reports and Technology Surveys.

Details on the availability of these publications may be obtained from:

SCIENTIFIC AND TECHNICAL INFORMATION OFFICE

NATIONAL AERONAUTICS AND SPACE ADMINISTRATION

Washington, D.C. 20546